Coordination Properties of Kläui's Tripodal Oxygen Donor toward Zirconium(IV)

Thomas R. Ward,*,† Séverine Duclos,† Bruno Therrien,† and Kurt Schenk‡

Chemistry and Biochemistry Department, University of Berne, Freiestrasse 3, CH-3012 Berne, Switzerland, and Crystallography Institute, University of Lausanne, BSP, CH-1015 Lausanne, Switzerland

Received February 10, 1998

The coordination properties of $[(\eta^5\text{-}C_5H_5)Co\{PR_2(O)\}_3]^-$ (R = OEt (L_{OEt}^-), Et (L_{Et}^-)) toward Zr(IV) have been investigated and compared to related cyclopentadienyl complexes. Addition of 2 equiv of L_{OEt}^- to $[ZrCl_4(THF)_2]$ yields labile $[Zr(L_{OEt})_2Cl_2]$ (**2**), which undergoes Arbuzov dealkylation to yield a dinuclear, seven-coordinate complex **1**. Reaction of **2** with MeLi yields the metathesis product LiL_{OEt}. Addition of 2 equiv of AgOTos to **2** affords octahedral $[Zr(L_{OEt})_2](OTos)_2$ (**3**). Reaction of $[ZrCpCl_3]$ with L_{OEt}^- leads to Cp^- displacement to give $[ZrL_{OEt}Cl_3]$ (**4**). Addition of 2 equiv of L_{Et}^- to $[ZrCl_4(THF)_2]$ yields octahedral $[Zr(L_{Et})_2](Cl)_2$ (**5**). Compounds **1**, **3**, **4**, and **5** have been characterized by X-ray crystallography.

Introduction

Early transition metal chemistry is dominated by systems incorporating cyclopentadienyl ligands. In the field of homogeneous catalysis, d^0 bent metallocene complexes $[Cp_2MX_2]^{n+}$, $Cp = \eta^5\text{-}C_5H_5$, display unrivaled catalytic properties. Although much effort has been invested to improve on existing metallocene catalysts, most useful systems to date still incorporate bent $\{Cp_2M\}$ fragments in many disguises.[1]

In a theoretical analysis, we recently showed that the unusual geometry (we call it edge-bridged tetrahedral EBT-5) adopted by $[Cp_2MX_3]$ complexes results from a distortion along a reversed-Berry pathway. This geometry is characterized by a planar MX_3 arrangment with acute X−M−X angles (symbolized 2α). From a structure-correlation analysis, we concluded that it is the *overlap* between the π-donor ligand L_π and the d^0-metal M which determines the efficiency of this distortion away from the trigonal-bipyramidal geometry and, thus, the acuteness of the X−M−X angle.[2] The π-orbitals of a cylindrical π-donor (L_π), which are responsible for the reversed-Berry distortion, have the same symmetry as the doubly degenerate orbitals of facial terdentate ligands. As such terdentate ligands have a very strong overlap with the metal, we reasonned that such ligands could force a d^0 metal into an EBT-5 geometry $[ML_2X_3]$ (see Scheme 1).

The anionic, Co(III)-based oxygen tripod $[CpCo\{PR_2(O)\}_3]^-$ (R = OEt or Et, abbreviated L_{OEt}^- and L_{Et}^-, respectively) developped by Kläui et al. has long been recognized as a cyclopentadienyl analogue.[3] Despite it hardness, the coordination chemistry of L_R^- with d^0 metals has received only little attention.[4−8] This prompted us to investigate the reactivity of Zr(IV) toward L_R^- and is the subject of this paper.

Results and Discussion

Reaction of $[ZrCl_4(THF)_2]$ with 2 equiv of NaL_{OEt} in THF at room temperature for 24 h yields, after NaCl filtration and solvent removal, a yellow powder. $^{31}P\{^1H\}$ NMR analysis of the crude reaction mixture indicates the presence of four different P nuclei in a 2:2:1:1 ratio, inconsistent with the expected $[Zr(L_{OEt})_2Cl_2]$ (**2**). Recrystallization from Et_2O affords X-ray-quality crystals in 75% yield. The low-temperature X-ray analysis reveals a dinuclear structure $[Zr_2(L'_{OEt})_4]$ (**1**) with seven-coordinate zirconiums and devoid of chlorides. This structure, reminiscent of that obtained by Nolan et al. for the reaction of YCl_3 with 2 equiv of NaL_{OEt} as well as Yeo et al. for $ZrCl_4$ with 2 equiv of L_{OMe}, arises from an Arbuzov dealkylation of two phosphonate alkyl groups for each Zr atom with concomitant ClEt evolution.[6,8] The resulting ligand bears a dianionic charge and can potentially act as a bridging ligand. Although all four ligands present in the dinuclear structure have lost an ethyl group as a result of the Arbuzov reaction, only two of these act as bridging ligands, resulting in a ZrO_7 coordination environment. The molecular structure of $[Zr_2(L'_{OEt})_4]$ (**1**) is depicted in Figure 1. Selected bond distances and angles are summarized in Table 1.

The above reaction can be conveniently followed by ^{31}P NMR. It appears that the L_{OEt}^-−Cl^- ligand exchange is rapid at room temperature (<5 min). The

† University of Berne.
‡ University of Lausanne.

(1) Lappert, M. F. *Comprehensive Organometallic Chemistry II*; Abel, E. W., Stone, F. G. A., Wilkinson, G., Eds.; Pergamon: Oxford, 1995; Vol. 4.
(2) Ward, T. R.; Bürgi, H.-B.; Gilardoni, F.; Weber, J. *J. Am. Chem. Soc.* **1997**, *119*, 11974.
(3) Kläui, W. *Angew. Chem.* **1990**, *102*, 661.
(4) Cho, I. Y.; Yeo, H. J.; Jeong, J. H.; Song, C. E. *Acta Crystallogr.* **1995**, *C51*, 2035.
(5) Kläui, W.; Müller, A.; Eberspach, W.; Boese, R.; Goldberg, I. *J. Am. Chem. Soc.* **1987**, *109*, 164.
(6) Liang, L.; Stevens, E. D.; Nolan, S. P. *Organometallics* **1992**, *11*, 3459.
(7) Banbery, H. J.; Hussain, W.; Evans, I. G.; Hamor, T. A.; Jones, C. J.; McCleverty, J. A.; Schulte, H.-J.; Engels, B.; Kläui, W. *Polyhedron* **1990**, *9*, 2549.
(8) Cho, I. Y.; Yeo, H. J.; Jeong, J. H. *Bull. Kor. Chem. Soc.* **1995**, *16*, 1244.

S0276-7333(98)00088-0 CCC: $15.00
Publication on Web 05/15/1998

Scheme 1. Steric and Electronic Factors Leading to a Reversed-Berry Distortion for d^0 Complexes

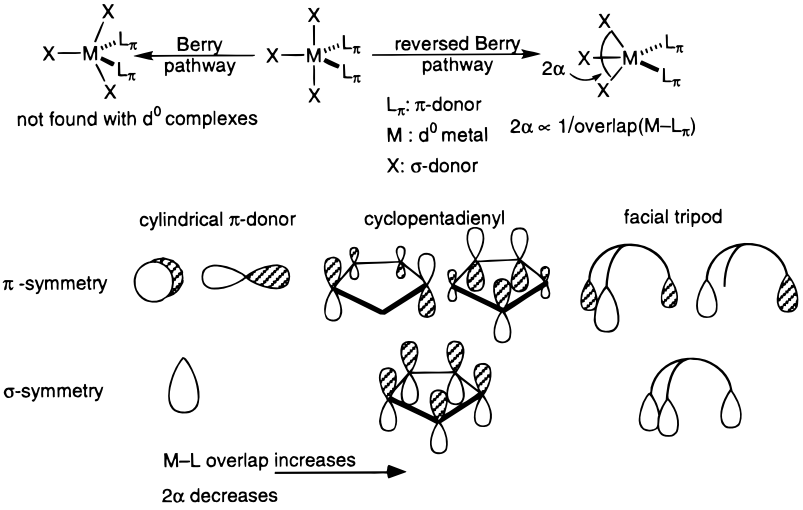

Table 1. Selected Interatomic Distances (Å) and Angles (deg) for $[Zr_2(L'_{OEt})_4]$ (1)[a]

Zr−O(21)	2.064(8)	P(2)−O(20)	1.465(11)
Zr−O(41)	2.100(9)	P(2)−O(21)	1.551(9)
Zr−O(40)#1	2.105(10)	P(3)−O(31)	1.513(9)
Zr−O(11)	2.130(8)	P(4)−O(40)	1.517(10)
Zr−O(51)	2.159(8)	P(4)−O(41)	1.537(9)
Zr−O(61)	2.224(9)	P(5)−O(51)	1.520(9)
Zr−O(31)	2.247(9)	P(6)−O(61)	1.523(9)
P(1)−O(11)	1.529(9)		

O(21)−Zr−O(41)	89.1(3)	O(41)−Zr−O(61)	77.8(3)
O(21)−Zr−O(40)#1	124.9(4)	O(40)#1−Zr−O(61)	147.6(3)
O(41)−Zr−O(40)#1	80.1(4)	O(11)−Zr−O(61)	75.4(3)
O(21)−Zr−O(11)	90.5(3)	O(51)−Zr−O(61)	76.7(3)
O(41)−Zr−O(11)	152.7(4)	O(21)−Zr−O(31)	77.2(3)
O(40)#1−Zr−O(11)	121.5(4)	O(41)−Zr−O(31)	130.6(4)
O(21)−Zr−O(51)	154.8(3)	O(40)#1−Zr−O(31)	70.6(3)
O(41)−Zr−O(51)	85.9(3)	O(11)−Zr−O(31)	75.7(4)
O(40)#1−Zr−O(51)	78.5(4)	O(51)−Zr−O(31)	124.0(3)
O(11)−Zr−O(51)	82.9(3)	O(61)−Zr−O(31)	141.5(3)
O(21)−Zr−O(61)	78.1(3)		

[a] Symmetry transformations used to generate equivalent atoms: #1 $-x, -y, -z$.

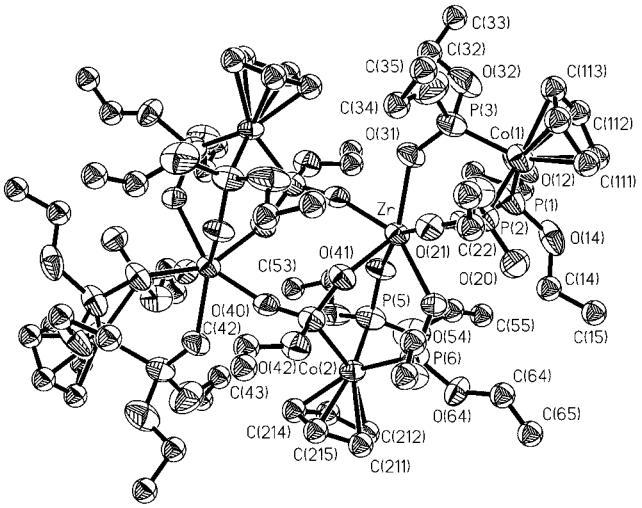

Figure 1. Molecular structure of $[Zr_2(L'_{OEt})_4]$ (**1**). Thermal ellipsoids are at the 50% probability level, and H atoms and disorder are deleted for clarity.

singlet at 120 ppm is tentatively assigned to $[Zr(L_{OEt})_2Cl_2]$ (**2**). All attempts to isolate this intermediate have yielded only impure material, contaminated with the rearranged product $[Zr_2(L'_{OEt})_4]$ (**1**). The Arbuzov rearrangment is complete within 18 h at room temperature.

In an attempt to isolate a $[Zr(L_{OEt})_2L_2]$ complex, a THF solution of $[ZrCl_4(THF)_2]$ was treated with 2 equiv of NaL_{OEt}, immediately followed by an alkylating agent, i.e., MeLi, $ZnEt_2$, EtMgBr. In all cases, by ^{31}P NMR we observed a ligand displacement (rather than a Cl^-/alkyl$^-$ exchange) from the zirconium to afford ML_{OEt} (M = Li, MgBr, ZnEt). This metathesis reaction is rationalized by the very high affinity of L_{OEt}^- for such metals, as reflected by their binding constants.[3]

Next, the in-situ-generated $[Zr(L_{OEt})_2Cl_2]$ (**2**) was treated with 2 equiv of [AgOTos] (Tos = *p*-$CH_3C_6H_4SO_2$). After AgCl filtration and solvent evaporation, the product was recrystallized from THF/hexane. All spectroscopic data were consistent with $[Zr(L_{OEt})_2(OTos)_2]$. An X-ray analysis of the latter, however, revealed a dicationic octahedral zirconium species, the tosylates acting as counterions: $[Zr(L_{OEt})_2](OTos)_2$ (**3**). This contrasts with Thewalt's recently published $[ZrCp_2(OTos)(H_2O)_2](OTos)$. In this latter case, the tosylates efficiently interact with the Zr (Zr−O = 2.169(5) Å).[9] The molecular structure and selected metrical data for $[Zr(L_{OEt})_2](OTos)_2$ (**3**) are presented in Figure 2 and Table 2, respectively.

Next, we reacted $[ZrCpCl_3]$ with 1 equiv of NaL_{OEt} in various solvents (THF, Et_2O, toluene). $^{31}P\{^1H\}$ NMR analysis of the crude mixture reveals a singlet at +119 ppm, consistent with η^3-coordination of L_{OEt}^- to zirconium. Recrystallization from CH_2Cl_2/C_6H_6 affords a pure crystalline product. ^1H and ^{13}C NMR spectra of the latter display a single cyclopentadienyl resonance with an integral of five rather than 10 as would be expected for $[ZrCpL_{OEt}Cl_2]$. The above spectroscopic data suggest that rather than displacing a chloride from $[ZrCpCl_3]$, L_{OEt}^- displaces η^5-Cp to afford $[Zr(L_{OEt})Cl_3]$ (**4**). This was confirmed by an X-ray analysis. The molecular structure of $[Zr(L_{OEt})Cl_3]$ (**4**) is depicted in Figure 3. Selected bond distances and angles are summarized in Table 3.

It is interesting to note that $[Zr(L_{OEt})Cl_3]$ does not undergo the Arbuzov dealkylation, even upon prolonged heating in THF. This suggests that only free rather

(9) Lasser, W.; Thewalt, U. *J. Organomet. Chem.* **1986**, *302*, 201.

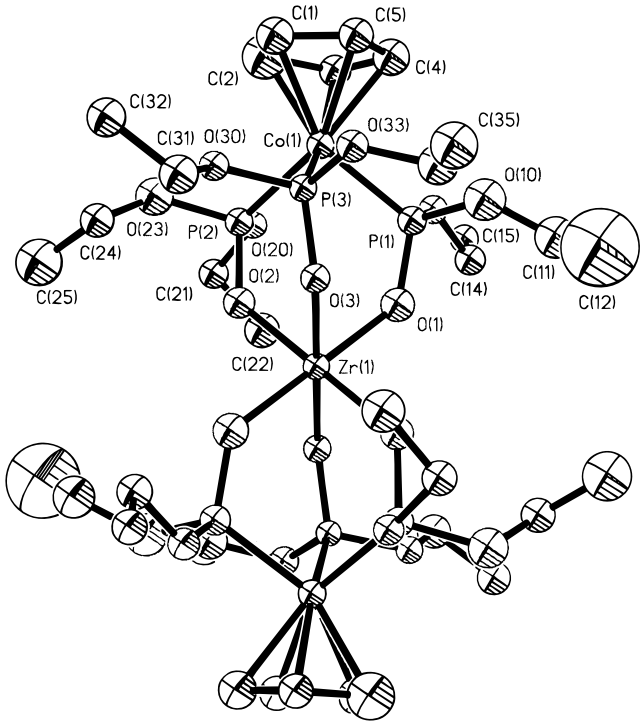

Figure 2. Molecular structure of $[Zr(L_{OEt})_2](OTos)_2$ (**3**). Thermal ellipsoids are at the 50% probability level. Only one molecule is displayed, and H atoms and OTos are deleted for clarity.

Table 2. Selected Interatomic Distances (Å) and Angles (deg) for $[Zr(L_{OEt})_2](OTos)_2$ (3)[a]

Zr(1)−O(1)#1	2.066(3)	O(1)#1−Zr(1)−O(2)#1	85.95(10)
Zr(1)−O(1)	2.067(3)	O(1)−Zr(1)−O(2)#1	94.05(10)
Zr(1)−O(2)	2.068(3)	O(2)−Zr(1)−O(2)#1	180.0
Zr(1)−O(2)#1	2.068(3)	O(1)#1−Zr(1)−O(3)#1	87.38(10)
Zr(1)−O(3)#1	2.077(3)	O(1)−Zr(1)−O(3)#1	92.62(10)
Zr(1)−O(3)	2.077(3)	O(2)−Zr(1)−O(3)#1	93.14(10)
P(1)−O(1)	1.544(3)	O(2)#1−Zr(1)−O(3)#1	86.86(10)
P(2)−O(2)	1.544(3)	O(1)#1−Zr(1)−O(3)	92.62(10)
P(3)−O(3)	1.548(3)	O(1)−Zr(1)−O(3)	87.38(10)
O(1)#1−Zr(1)−O(1)	180.0	O(2)−Zr(1)−O(3)	86.86(10)
O(1)#1−Zr(1)−O(2)	94.05(10)	O(2)#1−Zr(1)−O(3)	93.14(10)
O(1)−Zr(1)−O(2)	85.95(10)	O(6)#2−Zr(2)−O(6)	179.999(1)

[a] Two nearly identical independent molecules in the unit cell, only one considered in this table. Symmetry transformations used to generate equivalent atoms: #1 $-x, -y + 2, -z$; #2 $-x + 1, -y + 1, -z + 1$.

than coordinated chlorides can induce the rearrangement. The octahedral structure obtained for $[Zr(L_{OEt})_2](OTos)_2$ (**3**) suggests that the chlorides in $[Zr(L_{OEt})_2Cl_2]$ (**2**) are either loosely bound or dissociated.

To circumvent the Arbuzov rearrangment, we synthesized the alkyl-substituted ligand L_{Et}^- and reacted it with 0.5 equiv of $[ZrCl_4(THF)_2]$ in THF.[10] Upon coordination, the ^{31}P NMR signal shifts from 109 to 136 ppm. All spectroscopic data were consistent with $[Zr(L_{Et})_2Cl_2]$. Crystals grown from CH_2Cl_2 were submitted for X-ray analysis. The structure is octahedral around the zirconium, with a ZrO_6 environment: $[Zr(L_{Et})_2]Cl_2$ (**5**). The chlorides are fully dissociated (Zr−Cl = 7.250(1) Å). Despite the charge and the propensity of zirconium to afford complexes with coordination numbers higher than six, it thus appears that the tripodal ligands L_R^- are too bulky to allow eight coordination around Zr(IV). The molecular structure is presented in Figure 4. Selected bond distances and angles are summarized in Table 4.

(10) Kläui, W.; Eberspach, W.; Schwarz, R. *J. Organomet. Chem.* **1983**, *252*, 347.

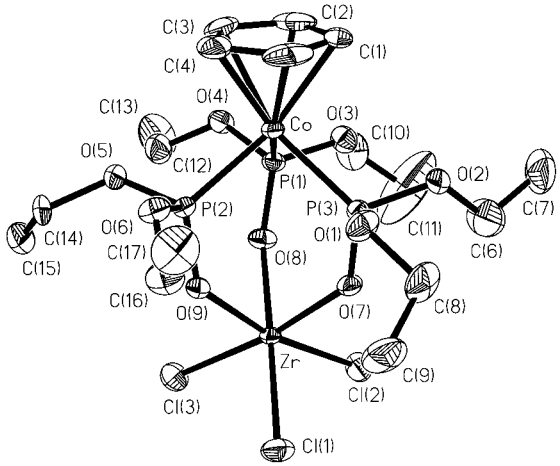

Figure 3. Molecular structure of $[Zr(L_{OEt})Cl_3]$ (**4**). Thermal ellipsoids are at the 50% probability level, and H atoms and solvents molecules are deleted for clarity.

Table 3. Selected Interatomic Distances (Å) and Angles (deg) for $[Zr(L_{OEt})Cl_3]$ (4)

Zr−O(7)	2.088(2)	Zr−Cl(3)	2.4414(10)
Zr−O(8)	2.094(2)	Zr−Cl(2)	2.4433(10)
Zr−O(9)	2.098(2)	Zr−Cl(1)	2.4460(9)
O(3)−C(10)	1.457(4)	P(1)−O(8)	1.537(2)
O(5)−C(14)	1.465(4)	P(2)−O(9)	1.539(2)
O(2)−C(6)	1.427(4)	P(3)−O(7)	1.537(2)
O(7)−Zr−O(8)	84.66(8)	O(9)−Zr−Cl(3)	90.54(6)
O(7)−Zr−O(9)	82.98(8)	O(7)−Zr−Cl(2)	89.33(6)
O(8)−Zr−O(9)	82.84(8)	O(8)−Zr−Cl(2)	89.51(6)
O(7)−Zr−Cl(3)	172.03(5)	O(9)−Zr−Cl(2)	169.61(6)
O(8)−Zr−Cl(3)	89.94(7)	Cl(3)−Zr−Cl(2)	96.50(4)
O(7)−Zr−Cl(1)	91.27(6)	Cl(3)−Zr−Cl(1)	93.51(4)
O(8)−Zr−Cl(1)	173.17(6)	Cl(2)−Zr−Cl(1)	95.95(4)
O(9)−Zr−Cl(1)	91.23(6)	P(1)−O(8)−Zr	136.55(13)
P(3)−O(7)−Zr	136.25(12)		

Outlook

Scheme 2 summarizes the reactivity of $[ZrCl_4(THF)_2]$ toward L_R^- (R = OEt, Et). In contrast to the Cp_2M-based chemistry, this chemistry is characterized by octahedral environments around zirconium. The Arbuzov rearrangment can be readily alleviated by use of L_{Et}^-, but the steric requirements of the tripod are such that the chorides are fully dissociated in $[Zr(L_{Et})_2]Cl_2$. Thus, L_R^- does not behave like a Cp^- analogue in the chemistry described here.

Experimental Section

General Considerations. NMR spectra were recorded on either a Varian XL 200 (^{31}P) or Brucker AM 300 (^1H,^{13}C) spectrometer. Chemical shifts are given in ppm and coupling constant in hertz. Signals are referenced against H_3PO_4 (^{31}P, external reference) and tetramethylsilane (^1H and ^{13}C, internal reference). Combustion analyses were carried out by Novartis, Basel. All experiments were carried out under a nitrogen atmosphere using standard Schlenk techniques. All solvents were distilled under nitrogen with standard desiccating agents. The compounds NaL_{OEt}[11] and NaL_{Et}[10] were prepared by literature methods.

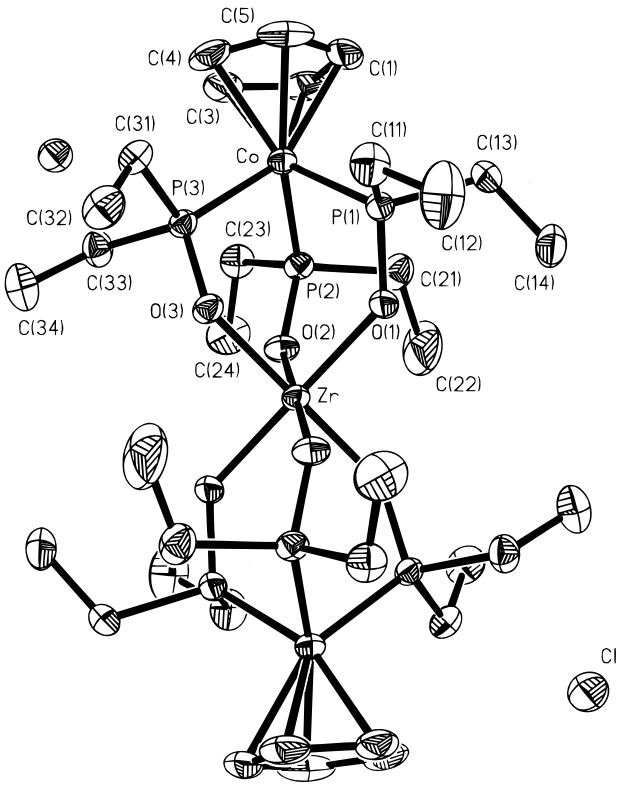

Figure 4. Molecular structure of $[Zr(L_{Et})_2]Cl_2$ (**5**). Thermal ellipsoids are at the 50% probability level, and H atoms are deleted for clarity.

Table 4. Selected Interatomic Distances (Å) and Angles (deg) for $[Zr(L_{Et})_2]Cl_2$ (5)[a]

Zr−O(1)	2.069(2)	P(1)−O(1)	1.563(2)
Zr−O(3)	2.072(2)	Zr−Cl	7.2495(9)
Zr−O(2)	2.073(2)	Co−P(3)	2.2064(9)
P(3)−O(3)	1.566(2)	Co−P(1)	2.2065(9)
P(2)−O(2)	1.568(2)	Co−P(2)	2.2178(9)
O(1)−Zr−O(2)	86.22(9)	O(3)−Zr−O(2)#1	94.00(8)
O(1)−Zr−O(3)	85.12(8)	P(1)−O(1)−Zr	133.77(13)
O(3)−Zr−O(2)	86.00(8)	P(2)−O(2)−Zr	133.19(13)
O(1)−Zr−O(2)#1	93.78(9)	P(3)−O(3)−Zr	132.11(12)
O(1)−Zr−O(3)#1	94.88(9)		

[a] Symmetry transformations used to generate equivalent atoms: #1 $-x+1, -y+1, -z+1$.

Structure Determination. X-ray diffraction data for **1**, **3**, and **5** were collected on a Siemens SMART CCD diffractometer[12] at low temperature using monochromatized graphite Mo Kα radiation (0.710 73 Å). The relevant structure determination parameters are summarized in Table 5. A complete hemisphere of data was scanned on $\omega = 0.3°$ with a run time of 20 or 60 s (unless otherwise stated) at the detector resolution of 512 × 512 pixels and a detector distance of 5.18 (for compounds **1** and **5**) and 5.93 cm (compound **3**). A total of 1271 frames were collected for each data set. Cell constants were obtained from 45 60 s frames. The collected frames were processed with the SAINT program[13] that automatically performs Lorentz and polarization corrections. Empirical absorption corrections were made using the XPREP program from the SHELXTL[14] software.

The data collection for compound **4** was carried out at 160 K on a Stoe ipds system equipped with Mo Kα radiation. Two hundred images with $\Delta\phi = 1°$ were exposed for 4 min each. The image plate was set to 80 mm, which resulted in a maximum 2θ of 48.4°. Reflection profiles varied from 9 to 21 pixels, and the effective mosaic spread was 0.009. An inspection of reciprocal space ascertained the diffraction figure to be exceptionally pure and to correspond to the cell given in Table 5. The crystal was bounded by {010} and {001} pinacoids and a {110} prism; a numerical absorption correction yielded an agreement factor for equivalent intensities of 0.0311 and transmission factors between 0.6411 and 0.7562. The intensities were further corrected for Lorentz and polarization effects.

Scheme 2. Summary of the Reactivity of $[ZrCl_4(THF)_2]$ toward L_R^-

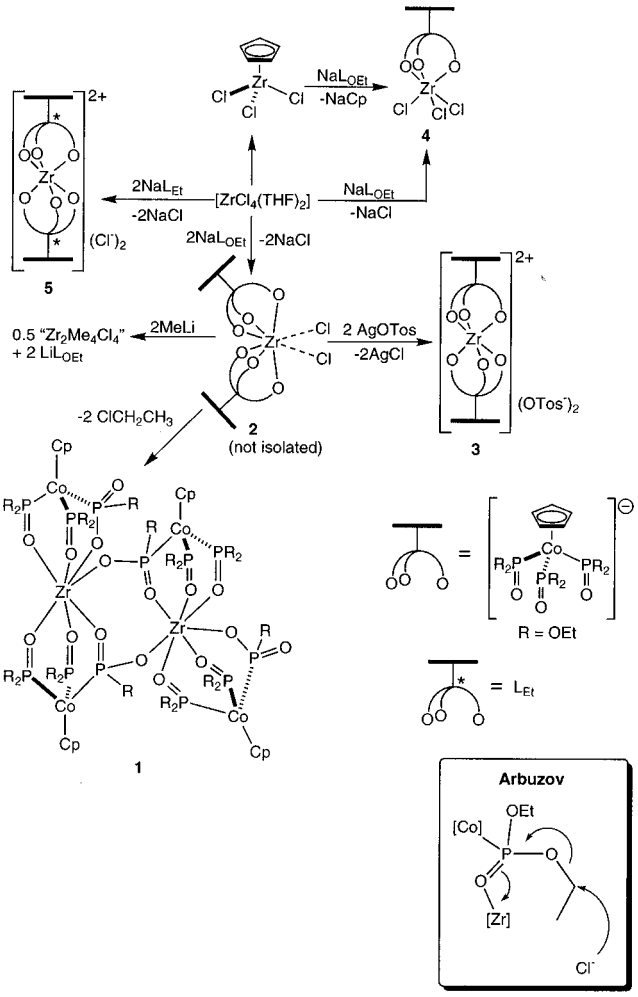

All structures were solved by direct methods, and the refinement was done by full-matrix least-squares of F^2 using SHELXL96[15] (β-test version). All non-hydrogen atoms were refined anisotropically, while hydrogen atoms (for compounds **1** and **5**), included at calculated positions, were refined in the riding model with group atomic displacement parameters. For compounds **3** and **4**, the hydrogens were kept riding on their associated carbon atoms and their isotropic displacement parameters were set to 1.2 or 1.5 times the U_{eq} of their associated carbons. Weights used were $[\sigma^2(F_o)^2]^{-1}$.

The slightly elevated residual densities and R_{int} value for **1** are a result of a poor quality crystal with disordered ethyl groups. To avoid that, we tried different crystals at different

(11) Kläui, W. *Z. Naturforsch.* **1979**, *34b*, 1403.
(12) *SMART, version 4. Software for the CCD Detector system*; Siemens Analytical Instruments Division: Madison, WI, 1995.
(13) *SAINT, version 4*; Siemens Energy and Automation Inc.: Madison, WI, 1995.
(14) *SHELXTL, version 5.03 (for Silicon Graphics). Program Library for Structure Solution and Molecular Graphics*; Siemens Analytical Instruments Division: Madison, WI, 1995.
(15) Sheldrick, G. M. *SHELXL96, Program for the Refinement of Crystal Structures*; University of Göttingen: Göttingen, Germany, 1996.

Table 5. Summary of the Crystallographic Data for Compounds 1, 3, 4, and 5

	1	3	4	5
formula	$C_{60}H_{120}Co_4O_{36}P_{12}Zr_2$	$C_{48}H_{84}Co_2O_{24}P_6S_2Zr$	$C_{20}H_{38}Cl_3CoO_9P_3Zr$	$C_{34}H_{70}Cl_2Co_2O_6P_6Zr\cdot 2CH_2Cl_2$
fw	2207.36	1504.22	771.91	1210.62
cryst syst	monoclinic	triclinic	monoclinic	triclinic
space group	$P2_1/n$	$P\bar{1}$	$P2_1/n$	$P\bar{1}$
a, Å	12.569(2)	13.857(5)	10.752(2)	10.7538(5)
b, Å	22.170(5)	15.254(5)	16.255(3)	10.9314(5)
c, Å	16.279(3)	17.875(5)	18.561(4)	13.6390(5)
α, deg		78.303(5)		97.496(1)
β, deg	94.11(1)	77.686(5)	102.93(3)	104.689(1)
γ, deg		64.709(5)		99.350(1)
V, Å^3	4524.6(1)	3311(2)	3162(1)	1505.4(1)
Z	2	2	4	1
ρ_{calcd}, mg/m^3	1.620	1.527	1.622	1.523
μ, mm^{-1}	1.230	0.937	1.302	1.356
F(000)	2272	1572	1572	708
cryst size, mm	0.08 × 0.10 × 0.10	0.09 × 0.22 × 0.30	0.22 × 0.22 × 0.09	0.09 × 0.18 × 0.40
T, K	203(2)	190(2)	180(2)	200(2)
exposure time/s	60	60		20
scan range, deg	$1.55 < \theta < 26.56$	$1.49 < \theta < 25.55$	$1.68 < \theta < 23.90$	$1.57 < \theta < 26.58$
total no. of data	10 418	13 859	19 311	7681
no. of unique obsd data	7308	10 142	4769	5483
no. of variables	604	752	335	326
goodness-of-fit	1.202	2.822	4.309	1.099
R(int)	0.0896	0.0271	0.0311	0.0284
final R_1[a] [$I > 2\sigma(I)$]	0.0984	0.0449	0.0290	0.0377
final wR_2[b] (all data)	0.2781	0.1026	0.0625	0.0955
max, min resid density, e Å^{-3}	1.745, −1.057	0.910, −0.548	0.506, −0.466	0.829, −0.671

[a] $R_1 = \sum||F_o| - |F_c||/\sum|F_o|$. [b] $wR_2(F_o^2) = \{\sum[w(F_o^2 - F_c^2)^2]/\sum[w(F_o^2)]\}$. $w = 1/[\sigma^2(F_o^2) + P^2 + P]$, where $P = (F_o^2 + 2F_c^2)/3$.

temperatures without any success. In our view, the accuracy of the stucture determination does not significantly detract from reality.

Synthesis of [$Zr_2(L'_{OEt})_4$] (1). A THF solution (2 mL) of NaL_{OEt} (0.25 g, 0.44 mmol) was added to $ZrCl_4(THF)_2$ (0.08 g, 0.22 mmol) in THF (3 mL). The mixture was stirred at room temperature for 24 h. After NaCl filtration, the solution was evaporated in vacuo to afford a yellow powder. Suitable cristals for X-ray diffraction were obtained by recrystallization from diethyl ether to yield [$Zr_2(L'_{OEt})_4$] (**1**; 0.36 g, 0.16 mmol, 75%). ^{1}H NMR ($CDCl_3$): δ 1.24 (m, 15H, C**H**$_3$), 3.70−4.22 (m, 8H, P(OC**H**$_2$−CH_3)$_2$), 4.44 (m, 2H, P(OC**H**$_2$−CH_3)), 5.10 (s, 5H, Cp). ^{13}C NMR ($CDCl_3$): δ 17.14, 17.80 (**C**H_3), 59.08, 59.94, 60.64, 60.74, 61.01, 61.11, 62.37, 63.51, 68.60 (**C**H_2), 90.46 (Cp). ^{31}P{^{1}H} NMR ($CDCl_3$): δ 80.98 (t, $^2J_{P-P}$ = 136.16 Hz, 1P, P(OCH_2−CH_3)), 80.68 (t, J_{P-P} = 135.36 Hz, 1P, P(OCH_2−CH_3)), 135.14 (d, 2P, P(OCH_2−CH_3)$_2$), 135.48 (d, 2P, P(OCH_2−CH_3)$_2$). Anal. Calcd for $C_{60}H_{120}O_{36}P_{12}Co_4Zr_2$: C, 32.65; H, 5.48; P, 16.84. Found: C, 32.68; H, 5.49; P, 17.45.

Synthesis of [$Zr(L_{OEt})_2Cl_2$] (2). A THF solution (3 mL) of NaL_{OEt} (0.51 g, 0.88 mmol) was added to a THF solution (5 mL) of $ZrCl_4(THF)_2$ (0.16 g, 0.44 mmol). After filtration, solvents were evaporated under reduced pressure to give a yellow powder. All attempts to purify the product yielded [$Zr(L_{OEt})_2Cl_2$] (**2**), contaminated with the rearranged product **1**. The crude product was, thus, directly used for the next step. ^{1}H NMR ($CDCl_3$): δ 1.28 (t,$^3J_{H-H}$ = 6.80 Hz, 18 H, C**H**$_3$), 4.11 (m, 12H, C**H**$_2$), 5.20 (s, 5H, Cp). ^{13}C NMR ($CDCl_3$): δ 17.13 (**C**H_3), 63.47 (**C**H_2), 90.95 (Cp). ^{31}P NMR (THF/C_6D_6): δ 120.

Synthesis of [$Zr(L_{OEt})_2$](OTos)$_2$ (3). A THF solution (8 mL) of [$Zr(L_{OEt})_2Cl_2$] (**2**) was treated with 2 equiv of AgOTos (0.24 g, 0.88 mmol) in THF (20 mL). The mixture was filtered, and the solvent was removed in vacuo to give [$Zr(L_{OEt})_2$](OTos)$_2$ (**3**) as a pale yellow powder. Slow diffusion of hexane through a THF solution of **3** affords yellow crystals in 80% yield (0.53 g, 0.35 mmol). ^{1}H NMR ($CDCl_3$): δ 1.29 (t,$^3J_{H-H}$ = 7.2 Hz, 18H, OCH_2−C**H**$_3$), 2.31 (s, 3H, C_{Ar}C**H**$_3$), 4.11 (m, 12H, OC**H**$_2$−CH_3), 5.28 (s, 5H, Cp), 7.09 (d, $^3J_{H-H}$ = 8.08 Hz, 2H, C_{Ar}**H**), 7.81 (d, 2H, C_{Ar}**H**). ^{13}C NMR ($CDCl_3$): δ 17.14 (**C**H_3−CH_2O), 21.94 (C_{Ar}**C**H_3), 63.67 (CH_3−**C**H_2O), 91.35 (Cp), 126.94, 128.95 (C_{Ar}). ^{31}P NMR ($CDCl_3$): δ 123. Anal. Calcd for $C_{48}H_{84}O_{24}P_6S_2Co_2Zr$: C, 38.33; H, 5.63. Found: C, 37.35; H, 5.64.

Synthesis of [$Zr(L_{OEt})Cl_3$] (4). A THF solution (2 mL) of NaL_{OEt} (0.20 g, 0.35 mmol) and $CpZrCl_3$ (0.09 g, 0.35 mmol) in THF (6 mL) were mixed and stirred at room temperature for 10 min. After filtration, solvents were evaporated in vacuo to give a yellow solid. The crude product was washed with hexane and recrystallized by adding C_6H_6 to a CH_2Cl_2 solution of [$Zr(L_{OEt})Cl_3$] (**4**; 0.18 g, 0.24 mmol, 70%). ^{1}H NMR ($CDCl_3$): δ 1.32 (t,$^3J_{H-H}$ = 6.98 Hz, 18H, C**H**$_3$−CH_2O), 4.20 (m, 12H, CH_3−C**H**$_2$O), 5.18 (s, 5H, Cp). ^{13}C NMR ($CDCl_3$): δ 17.15 (**C**H_3), 64.06 (**C**H_2), 90.73 (Cp). ^{31}P NMR ($CDCl_3$): δ 122. ^{31}P NMR (THF-d_8): δ 119. Anal. Calcd for $C_{17}H_{35}Cl_3O_9P_3CoZr$ (+0.5 C_6D_6 + 1H_2O): C, 30.29; H, 5.46. Found: C, 30.09; H, 6.29.

Synthesis of [$Zr(L_{Et})_2$]Cl_2 (5). A THF solution (3 mL) of NaL_{Et} (0.25 g, 0.52 mmol) was added to a THF solution (5 mL) of [$ZrCl_4(THF)_2$] (0.10 g, 0.26 mmol). After 5 min of stirring, the solution was filtered and evaporated in vacuo. The residue was then placed in a Soxhlet extractor and extracted under N_2 with CH_2Cl_2, affording yellow crystals suitable for X-ray analysis in 75% yield (0.20 g, 0.19 mmol). ^{1}H NMR ($CDCl_3$): δ 1.18 (m, 18H, C**H**$_3$), 1.99 (m, 6H, C**H**$_2$), 2.24 (m, 6H, C**H**$_2$), 5.02 (s, 5H, Cp). ^{13}C NMR ($CDCl_3$): δ 8.73 (**C**H_3), 31.95 (**C**H_2), 88.18 (Cp). ^{31}P NMR (CH_2Cl_2/C_6D_6): δ 136. Anal. Calcd for $C_{34}H_{70}Cl_2O_6P_6Co_2Zr$ (+CH_2Cl_2): C, 37.30; H, 6.40. Found: C, 36.90; H, 6.2.

Acknowledgment. T.R.W. thanks the Swiss National Science Foundation as well as the *Stiftung für Stipendien auf dem Gebiete der Chemie* for financial support; Novartis for elemental analyses, Christina Hoffmann for a preliminary X-ray data collection on **1**, Prof. A. Ludi for his hospitality, and Prof. W. Kläui for stimulating discussions.

Supporting Information Available: Tables of crystal data, atomic coordinates, anisotropic thermal parameters, bond lengths, and bond angles of compounds **1**, **3**, **4**, and **5** (21 pages). Ordering infomation is given on any masthead page. This information can also be retrieved via the Internet.

OM980088D